Electrodeposition of Ni–SiC nano-composite coatings and evaluation of wear and corrosion resistance and electroplating characteristics

M.R. Vaezi *, S.K. Sadrnezhaad, L. Nikzad

Advanced Materials Research Center, Materials and Energy Research Center, Karaj, Iran

Abstract

Ni–SiC nano-composite coatings with different contents of SiC nano-particulates were prepared by means of the conventional electrodeposition in a nickel-plating bath containing SiC nano-particulates to be co-deposited. The dependence of SiC nano-particulates amount in the nano-composite coatings was investigated in relation to the SiC concentration in bath, cathode current density, stir rate and temperature of plating bath and it is shown that these parameters strongly affected the volume percentage of SiC nano-particulates. The deposition efficiency with and without SiC nano-particulate in bath was studied. The morphology and phases of the electrodeposited nano-composite were studied. The wear behavior of the nano-composite coatings was evaluated on a ball-on-disk test. The corrosion behavior of the nano-composite coatings was evaluated in the solution of 0.5 M NaCl at room temperature. It was found that the cathodic polarization potential increased with increasing the SiC concentration in the bath. The microhardness and wear and corrosion resistance of the nano-composite coatings also increased with increasing content of the SiC nano-particulate in bath. The SiC distribution in the nano-composite coatings at low concentrations of SiC in bath was uniform across the coatings, but at high concentrations, SiC nano-particulates on the surface were agglomerated.
© 2007 Elsevier B.V. All rights reserved.

Keywords: Electrodeposition; Ni–SiC nano-composite coating; Corrosion resistance; Wear behavior

1. Introduction

Research into the production of nano-composite coatings by electrolytic co-deposition of fine particles with metal from plating baths has been investigated by numerous investigators [1–3]. Interest in electrodeposited nano-composites has increased substantially during the past two decades due mainly to the fact that nano-composite coatings can give various properties, such as wear resistance, high-temperature corrosion protection, oxidation resistance and self-lubrication, to a plated surface. Research on electrodeposition of nano-composite coatings has been attention directed towards the determination of optimum conditions for their production, i.e. current density, temperature, particle concentration and bath composition [1–5].

Nickel, being an engineering material, is the widely used metal matrix. Ni–SiC composites have been commercialized for the protection of friction parts, combustion engines and casting moulds [6,7]. The availability of nano-size particles in late 1990s and the resulting enhanced properties imparted by them to the coating have increased the interest in the production of nickel-based nano-composite coatings [8,9]. Quite a lot of researchers have studied the incorporation of micro/sub micro-SiC in nickel matrix [7,10–17]. Studies have also been reported on the influence of operating parameters on the co-deposition of nano-SiC [9,18–22]. Gyftou et al. have reported the co-deposition mechanism of micro and nano-SiC particles incorporated in nickel matrix [23]. The mechanical properties of Ni–SiC nano-composites from modified Watt's Bath have been studied by Zimmerman et al. [24].

As mentioned above, a lot of research work has been carried out on the effect of operating conditions on the mechanical properties of nano-composite coatings, but very few have examined the influence of electrochemical aspects such as determination of the cathodic efficiency on the co-deposition process and the properties of the resulting nano-composite coatings. This

* Corresponding author.
  E-mail addresses: vaezi9016@yahoo.com (M.R. Vaezi),
sadrnezhaad@sharif.edu (S.K. Sadrnezhaad),
leila_nikzad@yahoo.com (L. Nikzad).

paper presents results of research into the electrodeposition of Ni–SiC nano-composite coatings with particular reference to the electroplating parameters of the bath used. The microstructure and surface morphology of the composite coatings were investigated. The effects of the incorporated SiC on the cathodic efficiency of bath, corrosion and wear resistance of the nano-composite coatings were analyzed.

2. Experimental

The composition of the solution and operating parameters for electrodeposition are shown in Table 1. Analytical reagents and distilled water were used to prepare the plating solution. Prior to plating, the SiC nano-particulates of a mean diameter 50 nm (Kaier, Hefei, China) with concentration of 1–20 g L^{-1} were dispersed in the electrolyte in the presence of saccharine.

Cathodes, made of copper of a size 50 mm × 50 mm × 1 mm, were positioned in vertical plane with anode. A platinum plate of 40 mm × 40 mm was used as the anode. The distance between anode and cathode was 4 cm. Copper specimens with dimensions of 50 mm × 50 mm × 0.5 mm were used for the cathode efficiency determination.

Before each experiment, cathode was sequentially ultrasonically cleaned in ethanol, acetone and distilled water for 10 min, activated in 1:1 HCl for 30 s, washed in distilled water, and then immersed immediately in the plating bath to allow the electrodeposition of the target nano-composite coatings.

The electrochemical studies were performed on a model 273 A potentiostat/galvanostat device (EG & G Princeton Applied Research). The polarization curves of the electrolyte were recorded at a sweep rate of 0.1 mV/s. The Tafel curves were measured at a sweep rate of 0.01 mV/s in 0.5 M NaCl at room temperature.

Surface morphologies of nano-composite coatings were examined by scanning electron microscope (SEM) using a Philips model MV2300 operated at 25 kV. The chemical composition of the deposits was determined using the Kevex model energy dispersive X-ray spectroscopy (EDAX) system attached to the SEM. All chemical composition values are quoted in weight percent and represent the average of at least five measurements. X-ray diffraction (XRD) was used to determine the phase present and the preferred orientation of the deposits. A Philips Xpert-Pro X-ray diffractometer with a Cu Kα radiation ($\lambda = 1.5418$ Å) was employed to obtain XRD spectra using standard θ–2θ geometry. A computer-base search and match was used for phase identification.

The hardness of the nano-composites coatings was measured on a Vickers' microhardness instrument at an applied load of 50 g for 5 s. Five measurements were conducted on each sample and the results were averaged. The tribological behaviors of the electrodeposited nano-composites coatings reciprocally sliding against SAE52100 steel ball (φ 3 mm) were examined on a UMT-2MT tribometer in a ball-on-disk configuration. The sliding was performed at amplitude of 5 mm, a normal load of 1 N, and a frequency of 5 Hz.

3. Results and discussion

One of the purposes of this work was to find the dependence of the electrodeposited nickel percent on the different bath parameters and also the optimum conditions for the electrodeposition of nickel coatings. Fig. 1 shows the electrodeposited nickel weight percent as a function of current density at 30 and 60 °C. As can be seen in Fig. 1, with increasing current density from 20 to 70 mA/cm^2 at 30 °C the electrodeposited nickel percent is approximately constant (70%). An increase in current density at 60 °C (higher temperature) from 20 to 70 mA/cm^2 led to an increase in the electrodeposited nickel percent from 73 to 84%. Also, when the temperature of bath is increased from 30 to 60 °C at constant current density, the electrodeposited nickel percent will increase. Thus, the temperature of bath can promote the efficiency on the electrodeposition process of nickel and the effect of temperature is more significant than current density.

Fig. 2 indicates the variation in cathode efficiency of the nickel bath with current density for two temperatures, 30 and 60 °C. It can be seen that the cathode efficiency declines with the increase of current density. The efficiency is higher at 30 °C than at 60 °C at a given current density. This can be attributed to polarization at surface of cathode with increasing current density and temperature. The cathode efficiency at 30 °C varies from 75 to 45%.
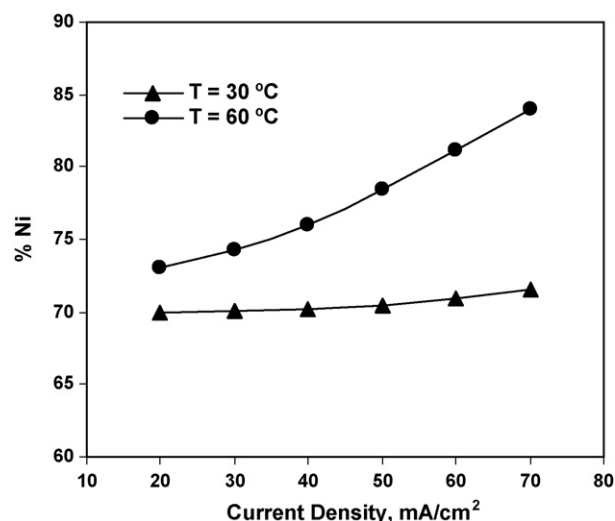
Table 1
Composition and deposition parameters of nano-composite bath used

Deposition parameters	Amount
NiSO$_4$	200 g/L
NiCl$_2$	40 g/L
Na$_3$C$_6$H$_5$O$_7$	50 g/L
H$_3$BO$_3$	30 g/L
SiC	1–20 g/L
Temperature	30 and 60 °C
pH	3
Current density	5–50 mA/cm^2
Magnetic stirring speed	600 rpm

Fig. 1. Chemical composition of matrix as a function of current density at 30 and 60 °C.

Fig. 2. The variation in cathode efficiency of the nickel bath with current density.

Fig. 3. The change in cathode efficiency with addition of SiC nano-particulates to bath at 30 °C.

The introduction of SiC nano-particulates to bath gives variation cathode efficiency. Fig. 3 shows the change in cathode efficiency with addition of the SiC nano-particulates to bath at 30 °C. When the SiC nano-particulates collide at the cathode surface, the conditions for deposit formation are established and so the cathode efficiency increases.

The SiC weight percent in composite coating as a function of SiC concentration, stirring rate, current density and the temperature of bath is shown in Fig. 4. Fig. 4a indicates that in constant
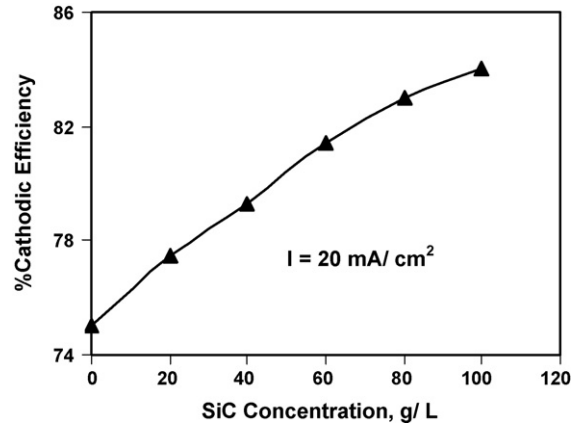
stirring rate, the weight percent of the SiC nano-particulates in the composite coating increases sharply with increasing the SiC nano-particulates content up to 5 g/L in the electrolyte. As the SiC concentration in the electrolyte surpasses 5 g/L, the weight percent of the SiC nano-particulates in the composite coating decreases (Fig. 4a). The results shown in Fig. 4a can be explained by the Guglielmi two-step adsorption model [1,2] where a higher particle concentration in the electrolyte increases the adsorption, thus resulting in a higher weight percent of SiC nano-particulates in composite coatings, while the decrease in the weight percent of the SiC nano-particulates at a concentration of SiC nano-particulates above 5 g/ L is attributed to the agglomeration of
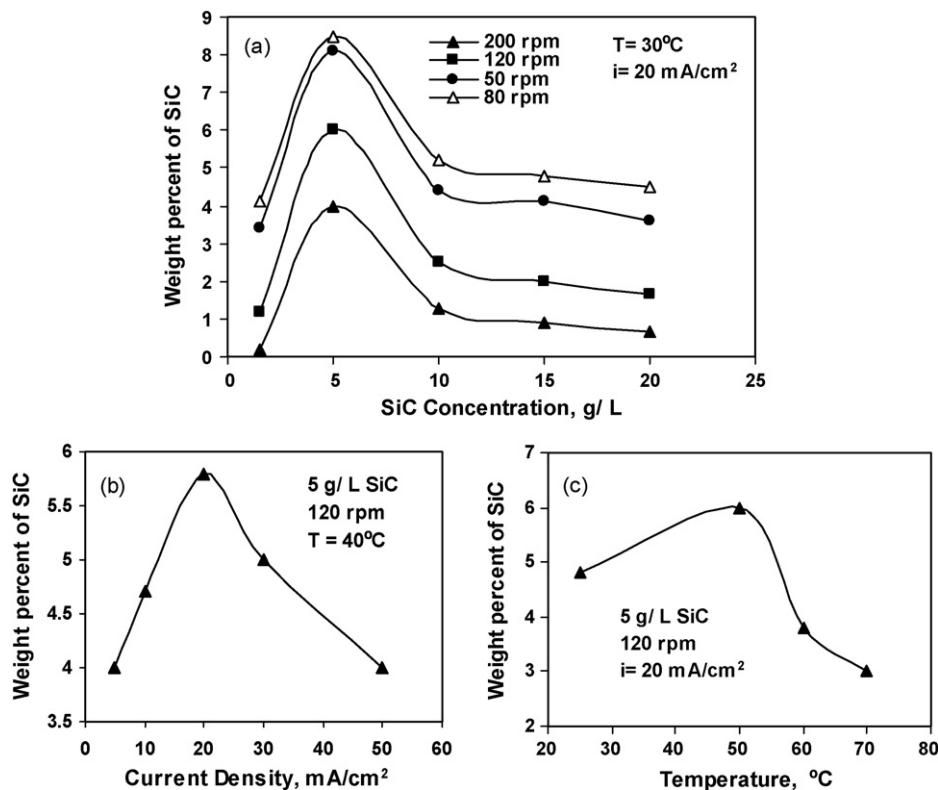

Fig. 4. The SiC nano-particulates weight percent as a function of SiC nano-particulates concentration and stirring rate (a), current density (b) and the temperature of bath (c).

the SiC nano-particulates in the electrolyte owing to their poor wettability. Increasing the stirring rate up to 120 rpm causes to increase the percent of SiC nano-particulates but when the stirring rate is too high, the decreasing trend of the weight percent is principally caused by the collision factor [25]. At a high-stirring rate, because of turbulent flow in bath, the SiC nano-particulates on the cathode surface are washed away and thus the SiC nano-particulates percent in composite coating decreases. In terms of the Foster model [26], with increasing of the stirring rate resulting in increasing the forces acting on the nano-particulates resting on the cathode surface, this decreases the weight percent of the SiC nano-particulates in the composite coating.

It is observed from Fig. 4b that the percent of SiC nano-particulates increases initially with the current density and reaches a maximum at 20 mA/cm^2. Beyond this current density, the weight percent of SiC nano-particulates decreases (see Fig. 4b). This result is in agreement with earlier observations by Wu et al. for Co–Ni–Al$_2$O$_3$ [27]. Before the maximum the increasing percent of SiC nano-particulates can be attributed to the increasing tendency for adsorbed particles to arrive in the cathode surface, which is consistent with Guglielmi model [28]. The process is controlled by the adsorption of the particles and the particle deposition is dominant. When current density is greater than 20 mA/cm^2, the decreasing trend can be explained by the fact that an increase in current density results in more rapid deposition of the metal matrix and fewer particles are embedded in the coating. Hence, the metal deposition dominates the deposition process.

Fig. 4c shows the percent of SiC nano-particulates as a function of the temperature of bath. It can be shown that the percent of SiC nano-particulates increases with the temperature of bath up to 50 °C. Below 50 °C, the activity of particulates increases with increasing the temperature of bath. However, as the temperature of bath is higher than 50 °C, the thermodynamic movement of the ions is greatly enhanced, which results in increasing the kinetic energy of particulates. According to the literature [29], increasing the temperature leads to the decrease in the adsorbability of the particulates and hence to decrease the overpotential of the cathode and the electric field, which makes it harder for the particulates to be embedded in the matrix and subsequently leads to a decrease in the weight percent of the SiC nano-particulates in the composite coating.

The dependence of the matrix composition on temperature at a cathode current density of 20 mA/cm^2 has been shown in Fig. 5. In Fig. 5, it was found that the presence of SiC nano-particulates in bath increases the weight percent of nickel in matrix of composite coatings.

The XRD method of Ni–SiC coatings is a suitable method to determine the phase kind and presence of SiC nano-particulates in the matrix. Fig. 6 shows the XRD diffractograms of pure nickel and Ni–SiC nano-compsite. The XRD pattern confirms that the electrodeposited nickel coating is composed of a mono-phase matrix (see Fig. 6a). Pure nickel deposit has exhibited an intense (2 0 0) diffraction line. This may be correlated with [1 0 0] texture associated to deposits with minimum hardness and maximum ductility. The intensity of the diffraction peaks of the nickel in the nano-composite coating is lower and the peak width is broader
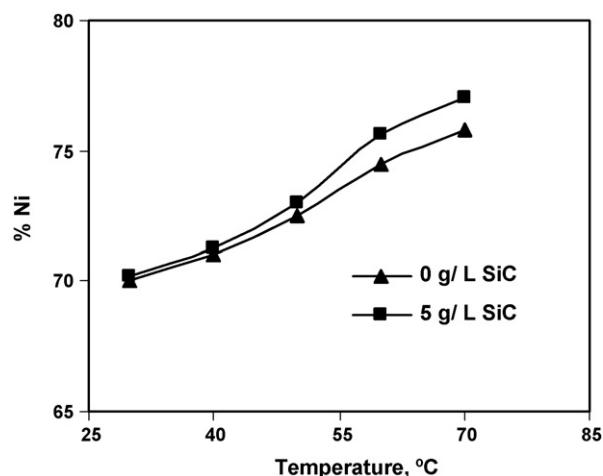

Fig. 5. The dependence of the matrix composition with temperature at the cathode current density of 20 mA/cm^2.

than that of the nickel coating (see Fig. 6b). This is attributed to the decrease in the grain size of the Ni–SiC nano-composite coating by the addition of SiC nano-particulates into the plating bath. Namely, the growth of the electrodeposited layer is a competition between the nucleation and crystal growth. SiC nano-particulates provide more nucleation sites and hence retard the crystal growth; subsequently the corresponding nickel matrix in the composite coating has a smaller crystal size. Pure nickel deposit exhibited a crystallite size of 28 nm, calculated from the XRD line broadening. The deposition of SiC (3 wt%) reduced the crystallite size to 11 nm (reference to (2 0 0) reflection).
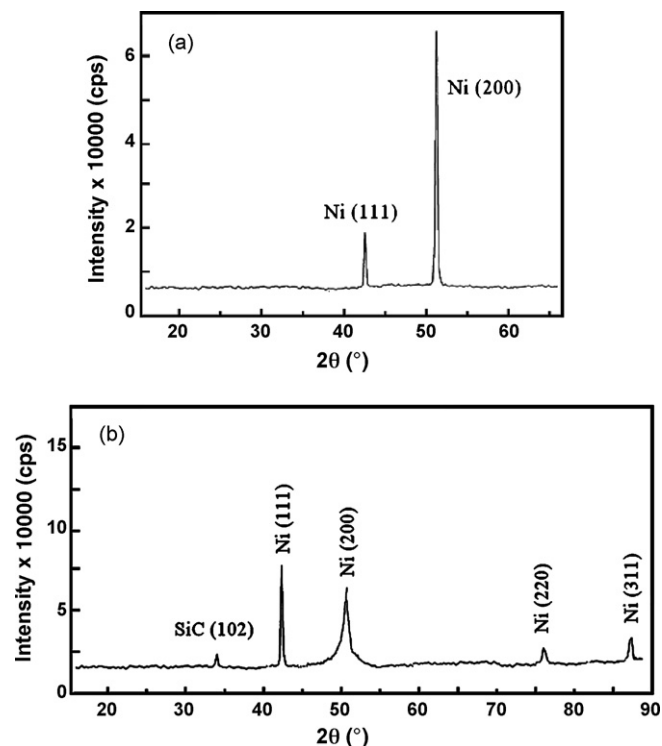

Fig. 6. XRD pattern of pure nickel deposit (a) and Ni–SiC nano-composite coating (b).

The Ni–SiC nano-compsite has exhibited (1 1 1), (2 2 0) and (3 1 1) diffraction lines with an attenuation of (2 0 0) line. This reinforcement of diffraction lines can be linked with the dispersed [2 1 1] orientation [30]. Thus the embedding of SiC nano-particulates in the nickel matrix has modified the texture from the soft [1 0 0] mode to the mixed preferred [2 1 1] mode [30]. Further, the incorporation of SiC nano-particulates in a nano-crystalline nickel matrix has also resulted in the increase in hardness from 260 to 450 VHN. The relation between the crystallite size and microhardness can be expressed by Hall-Petch relation, $H = H^0 + kd^{-1/2}$ [31] where k is a constant known as the Hall-Petch stress intensity factor, d crystallite size, H microhardness and H^0 is the hardness of the material. This is based on the concept that grain boundaries act as barriers to the motion of dislocations by forming dislocation pile-ups at grain boundaries, resulting in hard deposits. The reduction in grain size and change in structure of nickel crystallites may be linked to the fact that SiC nano-particulates change the catholyte composition due to adsorption of H^+. This results in the localized alkalization of cathode/ electrolyte interface leading to [2 1 1] mode. It also perturbs the crystal growth by increasing the number of nucleation sites and consequently a reduction in the crystallite size occurs.

The surface morphology of the coatings analyzed by SEM is given in Fig. 7. The figure reveals that the pure nickel deposit has exhibited irregular polyhedral crystals. The incorporation of SiC nano-particulates has modified the surface to particulate like crystals. The change in the morphology can be associated to the change from preferred orientation to random oriented composite deposits. EDX analysis revealed the uniform distribution of SiC in the composite. In addition, many nodular agglomerated grains are seen on the nano-composite coating surface (Fig. 7c). It is supposed that the SiC nano-particulates of a uniform distribution and agglomeration to some extent may contribute to increase the wear resistance of the Ni–SiC nano-composite coating.

Fig. 8 shows the variation in the microhardness and wear rate of the Ni–SiC nano-composite coatings with the content of SiC nano-particulates. It is seen that the Ni–5% SiC nano-composite coating has a maximum hardness and minimum wear rate. The microhardness of the nano-composite coatings increases with increasing weight percent of the SiC nano-particulate. The increase in the microhardness and the decrease in the wear rate of the Ni–SiC nano-composite coatings as compared to the nickel coating is rationally understood, since the SiC nano-particulates deposited in the nickel matrix could restrain the growth of the nickel grains and the plastic deformation of the matrix under a loading, by way of grain fining and dispersive strengthening effects. The grain fining and dispersive strengthening effects become stronger with increasing SiC nano-particulates content, thus the microhardness and wear resistance of the Ni–SiC nano-composite coatings increase with increasing SiC nano-particulates content.
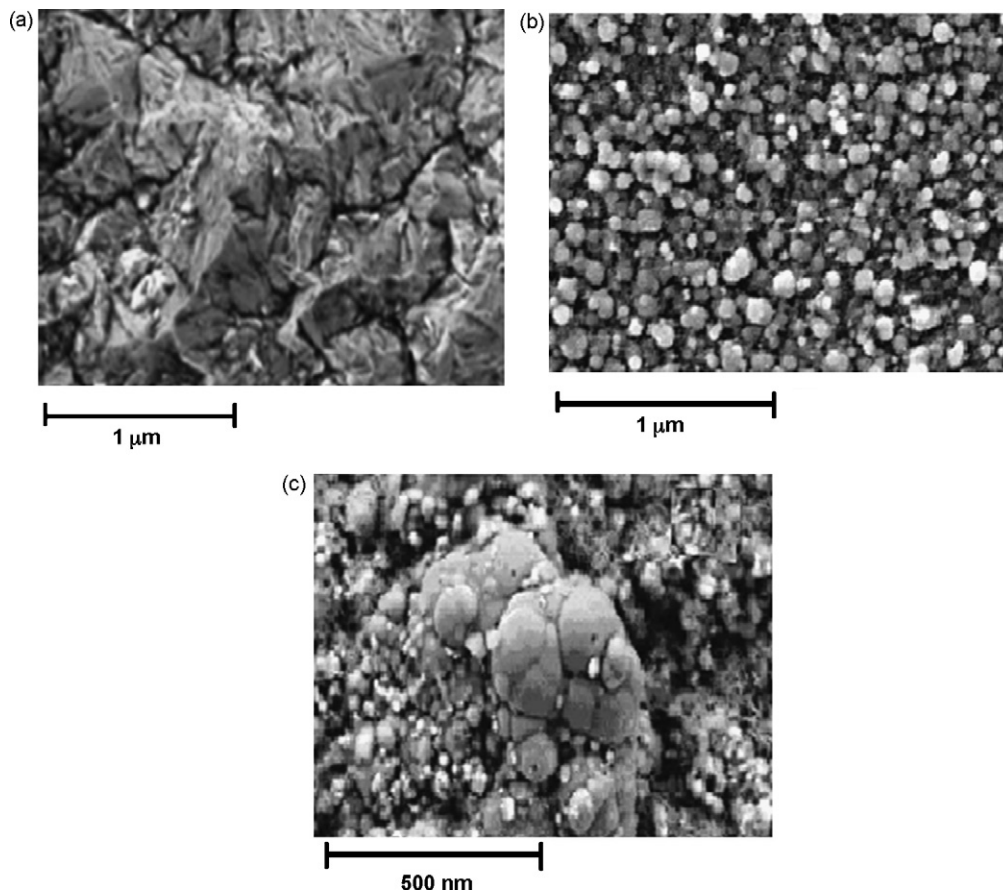

Fig. 7. SEM morphology of nickel coating (a) and Ni–SiC nano-composite coating (b and c).
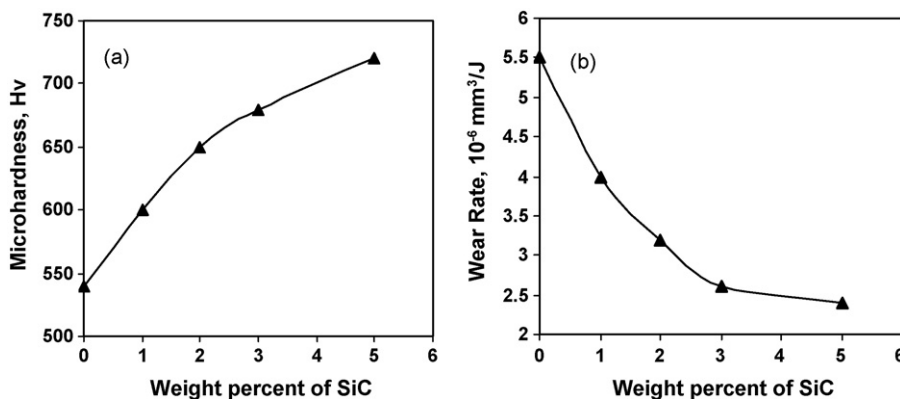
Fig. 8. Microhardness (a) and wear rate (b) of the Ni–SiC nano-composite coating vs. weight percent of SiC nano-particulates.

The cathodic polarization curves of the Ni–SiC electrolytes containing different concentrations of SiC nano-particulates has been shown in Fig. 9. It is seen that the addition of SiC nano-particulates to the electrolyte causes the reduction potential of nickel to shift towards larger negatives, but the slope of the reduction curve keeps unchanged. The shift to a lower value in the reduction potential is attributed to a decrease in the active surface area of the cathode, owing to the adsorption of the SiC nano-particulates, and may also relate to the decrease in the ionic transport by the SiC nano-particulates, which does not significantly affect the electrochemical reaction mechanism.

Fig. 10 shows the anodic polarization curves for nickel and Ni–SiC nano-composite coating in 0.5 M NaCl solutions. Both of them show an active-passive transition by anodic polarization, but the corrosion potential of Ni–SiC nano-composite coating is more positive than that of nickel coating. For Ni–SiC nano-composite coating, the polarization curve shows a relatively wide passive region and smaller passive current density than that of nickel coating. This indicates that the Ni–SiC nano-composite coating has better corrosion resistance than the nickel coating. The SiC nano-particulates were embedded in the nickel matrix and filled in crevices, gaps and micron holes. These SiC nano-particulates act as inert physical barriers to the initiation and development of defect corrosion, hence improve the corrosion resistance of the coating.
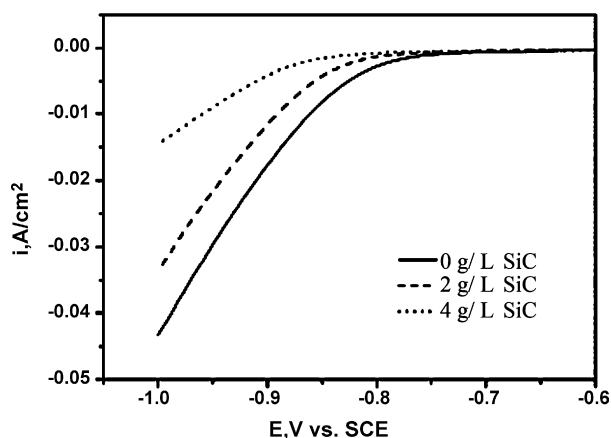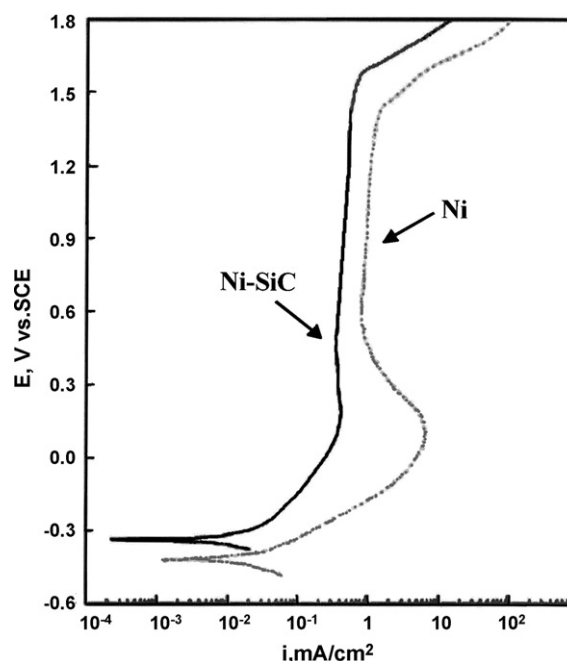

Fig. 10. Cathodic polarization curves of nickel and Ni–SiC nano-composite coating (containing 3% SiC) in 0.5 M NaCl solution.

4. Conclusion

The electrodeposited nickel percent depends on current density and temperature. The current density and SiC content in solution influence the cathode efficiency; with decrease of current density or increase of the SiC content in bath, the cathode efficiency increases. SiC nano-particulates can be successfully co-deposited with nickel by electrodeposition. The cathodic polarization potential of the Ni–SiC electrolyte increases with increasing SiC concentration in the plating bath, but the SiC nano-particulates do not significantly affect the electrodeposition process of the nickel coating. It is recommended to prepare the Ni–SiC nano-particulates composite coating of the largest weight percent of SiC nano-particulates by plating in the bath containing 5 g/ L SiC nano-particulates at a temperature of 30 °C, current density of 20 mA/cm^2, and a stirring rate of 120 rpm. The incorporation of the SiC nano-particulates leads to

Fig. 9. Cathodic polarization curves for the deposition of Ni–SiC at different concentrations of SiC nano-particulates in the bath.

the changes in the morphology, microhardness and wear resistance of the nano-composite coatings as compared to the nickel coatings. The Ni–SiC nano-composite coatings have higher microhardness and better wear resistance than the nickel coating, which is attributed to the grain-fining and dispersive strengthening effects of the deposited hard SiC nano-particulates. The Ni–SiC nano-composite coating has better corrosion resistance than the nickel coating.

References

[1] M. Ghouse, M. Viswanathan, Met. Finish. 57 (1980).
[2] M. Ghouse, M. Viswanathan, E.G. Ramachandran, Met. Finish. 31 (1980).
[3] M. Ghouse, E.G. Ramachandran, Met. Finish. 85 (1981).
[4] T.W. Tomaszewski, Trans. Inst. Met. Finish. 54 (1976) 45.
[5] P.J. Sonnenwald, W. Visscher, E. Barendreht, J. Appl. Electrochem. 20 (1990) 563.
[6] L. Benea, P.L. Bonora, A. Borello, S. Martelli, Wear 249 (2002) 995.
[7] S.H. Yeh, C.C. Wan, J. Appl. Electrochem. 24 (1994) 993.
[8] E.A. Pavlatou, M. Stroumbouli, P. Gyftou, N. Spyrellis, J. Appl. Electrochem. 385 (2006).
[9] C.T.J. Low, R.G.A. Wills, F.C. Walsh, Surf. Coat. Technol. 201 (1/2) (2006) 371–383.
[10] P. Gyftou, M. Stroumbouli, E.A. Pavlatou, P. Asimidis, N. Spyrellis, Electrochim. Acta 50 (2005) 4544.
[11] N.K. Shrestha, M. Masuko, T. Saji, Wear 254 (2003) 555.
[12] E. Rabinowicz, Wear 100 (1984) 533.
[13] S. Shawki, Z. Abdel Hamid, Aircr. Eng. Aerosp. Technol. 69 (5) (1997) 432.
[14] R.P. Socha, K. Laajalehto, P. Nowak, Colloids Surf. A: Physicochem. Eng. Aspects 208 (2002) 267.
[15] C.S. Lin, K.C. Huang, J. Appl. Electrochem. 34 (2004) 1013.
[16] I. Garcia, A. Conde, G. Langelaan, J. Fransaer, J.P. Celis, Corros. Sci. 45 (2003) 1173.
[17] R.P. Socha, P. Nowak, K. Laajalehto, J. Vayrynen, Colloids Surf. A: Physicochem. Eng. Aspects 235 (2004) 45.
[18] M.-D. Ger, Mater. Chem. Phys. 87 (2004) 67.
[19] C.T.J. Low, R.G.A. Wills, F.C. Walsh, Surf. Coat. Technol. 201 (1-2) (2006) 371–383.
[20] S.-C. Wang, W.-C.J. Wei, Mater. Chem. Phys. 78 (2003) 574.
[21] B. Lidia, P.L. Bonora, A. Borello, S. Martelli, F. Wenger, P. Ponthiaux, J. Galland, Solid State Ionics 151 (2002) 89.
[22] M. Lekka, N. Kouloumbi, M. Gajo, P.L. Bonora, Electrochim. Acta 50 (2005) 4551.
[23] C.F. Windisch Jr., K.F. Ferris, J. Gregory, Exarhos, J. Vac. Sci. Technol. A 19 (2001).
[24] A.F. Zimmerman, G. Palumbo, K.T. Aust, U. Erb, Mater. Sci. Eng. A 328 (2002) 137.
[25] S.H. Yeh, C.C. Wan, Plat. Surf. Finish. 84 (1997) 54.
[26] J. Foster, B. Cameron, Trans. Inst. Met. Finish. 54 (1976) 178.
[27] G. Wu, N. Li, D.R. Zhou, K.C. Mitsuo, Surf. Coat. Technol. 176 (2003) 157.
[28] N. Guglielmi, J. Electrochem. Soc. 119 (8) (1972) 1009.
[29] S.K. Sadrnezhaad, Kinetics Processes in Materials Engineering and Metallurgy, 2nd ed., Amir Kabir Pub. Inst., Tehran, Iran, 2004 (in Persian).
[30] P.A. Gay, P. Berçot, J. Pagetti, Surf. Coat. Technol. 140 (2001).
[31] F. Erler, C. Jakob, H. Romanus, L. Spiess, B. Wielage, T. Lampke, S. Steinhouser, Electrochim. Acta 48 (2003) 3063.